

# Effect of diffusion and competitive dynamics in the simplest discontinuous absorbing transition model

Salete Pianegonda

*Instituto de Física, Universidade Federal do Rio Grande do Sul,  
Caixa Postal 15051, CEP 91501-970, Porto Alegre, RS, Brazil*

Carlos E. Fiore

*Instituto de Física, Universidade de São Paulo, Caixa Postal 66318  
05315-970 São Paulo, SP, Brazil*

(Dated: December 7, 2024)

Contact processes (CP) with particle creation requiring a minimal neighborhood (called restrictive CPs) present a novel sort of discontinuous absorbing transitions, that remain unchanged under the inclusion of distinct ingredients, such as distinct lattice topologies and particle annihilations. Here, we give a further step by addressing the effect of diffusion and a competitive dynamics, in order to weakening the phase coexistence. Models have been studied via mean-field theory (MFT) and numerical simulations. Results point out in opposite directions. Whenever the competitive dynamics suppresses the phase coexistence for intermediate and large rates, the diffusion maintains a discontinuous transition for all diffusion values. This result contrasts with very recent studies based on a Langevin approach, in which limited diffusion suppresses the phase coexistence. Also, unlike results by Guo et al. (J. Chem. Phys. **130**, 074106 (2009)), all discontinuous transitions take place in a single and well defined point, in similarity with those yielded in equilibrium systems. MFT predictions are in qualitative agreement with numerical results. In all cases, finite size scalings similar to first-order equilibrium phase transitions have been found, shedding light on a general scaling for discontinuous nonequilibrium phase transitions.

## I. INTRODUCTION

Nonequilibrium phase transitions into absorbing states describe several problems, such as wetting phenomena, spreading of diseases, chemical reactions and others [1, 2]. Notwithstanding a large effort in the last years, including experimental verifications [3–5], a complete characterization of absorbing phase transitions as well as the establishment of distinct universality classes are still lacking. In most cases, phase transitions are second-order and belong to the directed percolation (DP) universality class [2, 6, 7]. Despite some classical examples of discontinuous absorbing transitions [8], more recently they have attracted great interest by the search of minimal ingredients for their occurrence. In particular, it is argued that the particle creation requiring a minimal neighborhood (larger than 1 particle) for creating a new species [9–12] is responsible for shifting the phase transition, from continuous to discontinuous. In the simplest model [11], the transition rates do not depend neither on the particle neighbors orientation nor their numbers (provided that is greater than 1). The phase coexistence, induced by this mildly change, remains unaffected under the inclusion of distinct creation [9–12] and annihilation rules [12] and also study in lattice topologies [13], even violating available theoretical predictions [14].

Although critical transitions are characterized in universality classes that only depend on general ingredients, the inclusion of some dynamics, such as spatial disorder and particle diffusion, can cause drastic changes in the critical behavior [2]. Their effect for first-order phase transitions is still much less understood. The few avail-

able studies have shown that the inclusion of spatial disorder in a given variant of restrictive model destroys the phase coexistence, giving rise to a continuous transition that belongs to a new universality class [15]. A similar scenario of scarce results also holds for the outcome of diffusion, whose available studies provide distinct findings. Very recent analysis of a Langevin-like approach reported that whenever strong diffusions maintain a phase coexistence, limited rates suppress it, giving rise to DP critical transition [16]. On the other hand, results of the restrictive CP by Guo et al. [10], in which the transition rates depend on specific particle displacements, have shown that the increase of diffusion destroys the generic two-phase coexistence, but not the discontinuous transition.

With these ideas in mind, we scrutinize the influence of different dynamics in the simplest restrictive CP version, in order to address the robustness of discontinuous absorbing transitions. Our study includes the effect of particle diffusion and a weakening mechanism of the restrictive interaction. The former dynamics analysis is undertaken by rising three fundamental points: what is the effect of strong and limited diffusion in a minimal lattice model? does it suppress the phase coexistence? how do results compare with those from Refs. [10, 16]? We consider three diffusion values, exemplifying the low, intermediate and large regimes. The second ingredient is accomplished by including the competition with usual CP dynamics (whose transition is second-order). Although a critical DP transition is expected in the regime of less frequent restrictive interactions, we tackle on answering similar questions than for the diffusive case: is the phase coexistence suppressed for limited or large non-restrictive

interactions? how does the tricritical point (separating phase coexistence from critical transition) compare with the results [17] of the model by Guo et al. [10]? In other words, does a simplified model change the location of tricritical point?

Models will be studied via MFT and distinct sort of numerical simulations. Results show that whenever the weakening dynamics suppresses the phase coexistence for intermediate and large rates, the diffusion maintains a discontinuous transition for all diffusion values. In all cases, the discontinuous transitions are signed by finite size scaling behavior similar to equilibrium phase transitions. Since there is no theory for the nonequilibrium case, our results shed light over a general finite-size scaling for them.

## II. MODELS

Let us consider a system of interacting particles placed on a square lattice of linear size  $L$ . To each site is attached an occupation variable  $\eta_i$  that assumes the value 0 (1) whenever sites are empty (occupied). The former model is defined by the following interaction rules: particles are annihilated with rate  $\alpha$  and are created with rate 1 in empty sites only if its number of nearest neighbor particles  $nn$  is larger than 1 ( $nn \geq 2$ ). There is no particle creation if  $nn \leq 1$ . Besides the above processes, with probability  $D$  a particle hops to one of its nearest neighbor sites provided it is empty.

The second study takes into account the above annihilation process, but with probability  $p$  the creation requires at least  $nn \geq 1$  neighbor particles and with complementary probability  $1 - p$  the above restrictive dynamics requiring  $nn \geq 2$  is selected. The extreme cases  $p = 0$  and  $p = 1$  reduce to the restrictive [11] and the usual CP, respectively, whose transitions are discontinuous and continuous yielding at  $\alpha_c = 0.60653(1)$  [18], respectively.

In both variants, a phase transition separates an active regime (stable for low  $\alpha$ ) from an absorbing phase at a transition point  $\alpha_0$ . The order parameter is the particle density  $\rho$ , in such a way that  $\rho = 0$  in the absorbing state and  $\rho \neq 0$  in the active phases.

## III. MEAN-FIELD ANALYSIS

Let the symbols  $\bullet$  and  $\circ$  to represent occupied and empty sites, respectively. From the above dynamic rules, we derive relations for the time evolution of relevant quantities. Since the diffusion conserves the particle number, it is required to take into account at least correlations of two sites for developing mean-field treatments and hence two equations are needed. In particular, by identifying the system density  $\rho$  as the one-site probability  $\rho = P(\bullet)$  and considering the two-site correlation

$u = P(\bullet\bullet)$ , from the previous models rules we obtain the following relations

$$\frac{d\rho}{dt} = 4P(\circ\bullet\bullet\bullet) + 2P(\circ\bullet\circ\bullet) + 4P(\circ\bullet\circ\bullet\bullet) + P(\circ\bullet\bullet\bullet\bullet) - \alpha P(\bullet) \quad (1)$$

$$\begin{aligned} \frac{du}{dt} = & (1 - D)[-2P(\circ\bullet\bullet\bullet) - P(\circ\bullet\bullet\bullet\bullet)] \\ & - \alpha P(\circ\bullet) + \alpha P(\bullet\bullet) + D[6P(\bullet\bullet) - 6P(\circ\bullet\bullet)] \end{aligned} \quad (2)$$

for the model 1 and

$$\begin{aligned} \frac{d\rho}{dt} = & (1 - p)[4P(\circ\bullet\bullet\bullet\circ) + 2P(\circ\bullet\circ\bullet\circ) + 4P(\circ\bullet\circ\bullet\bullet)] \\ & + P(\circ\bullet\bullet\bullet\bullet) + pP(\circ\bullet) - \alpha P(\bullet) \end{aligned} \quad (3)$$

$$\begin{aligned} \frac{du}{dt} = & (1 - p)[-2P(\circ\bullet\circ\bullet\bullet) - P(\circ\bullet\bullet\bullet\bullet)] \\ & + p \left[ -\frac{3}{2}P(\circ\bullet\bullet) + \frac{1}{2}P(\circ\bullet) \right] \\ & - \alpha P(\circ\bullet) + \alpha P(\bullet\bullet) \end{aligned} \quad (4)$$

for the model 2. The symbol  $P(\eta_0, \eta_1, \eta_2, \eta_3, \eta_4)$  denotes the probability of finding the central site in the state  $\eta_0$  and its four nearest neighbors in the states  $\eta_1, \eta_2, \eta_3$  and  $\eta_4$ .

The pair mean-field approximation consists of rewriting the  $n$ -site probabilities ( $n > 2$ ) as products of two-site and one-site probabilities in such a way that

$$P(\eta_0, \eta_1, \dots, \eta_{n-1}) \simeq \frac{P(\eta_0, \eta_1)P(\eta_0, \eta_2)\dots P(\eta_0, \eta_{n-1})}{P(\eta_0)^{n-2}}. \quad (5)$$

Using this approximation in the above equations we obtain

$$\frac{d\rho}{dt} = \frac{6u^2}{(1-\rho)} - \frac{8u^3}{(1-\rho)^2} + \frac{3u^4}{(1-\rho)^3} - \alpha\rho \quad (6)$$

$$\begin{aligned} \frac{du}{dt} = & (1 - D) \left[ -\frac{2u^3}{(1-\rho)^2} + \frac{u^4}{(1-\rho)^3} - 2\alpha u + \alpha\rho \right] \\ & + D \left[ 6u - \frac{6u^2}{\rho(1-\rho)} \right] \end{aligned} \quad (7)$$

for the model 1 and

$$\frac{d\rho}{dt} = (1 - p) \left[ \frac{6u^2}{(1-\rho)} - \frac{8u^3}{(1-\rho)^2} + \frac{3u^4}{(1-\rho)^3} \right] + pu - \alpha\rho \quad (8)$$

$$\begin{aligned} \frac{du}{dt} = & (1 - p) \left[ -\frac{2u^3}{(1-\rho)^2} + \frac{u^4}{(1-\rho)^3} \right] \\ & + p \left[ \frac{u}{2} - \frac{3u^2}{2(1-\rho)} \right] - 2\alpha u + \alpha\rho \end{aligned} \quad (9)$$

for the model 2.

Since the steady solutions are obtained by taking  $\frac{d\rho}{dt} = \frac{du}{dt} = 0$  for the models 1 and 2, we locate the transition point and the order of transition by solving a system of two coupled equations for a given set of parameters  $(\alpha, D)$  and  $(\alpha, p)$ , respectively. The existence of a spinodal behavior (with  $\rho$  increasing by raising  $\alpha$ ) signals a discontinuous transition and otherwise it is continuous. Fig. 1 (a) shows the phase diagram for distinct diffusion rates. For all values of  $D$ , mean-field results predict discontinuous transitions separating the absorbing and the active phases. However, as  $D$  increases, the transition point moves to larger values and the active phase becomes less dense. For example, for  $D = 0.1$  and  $D = 0.9$  (inset), the active phases have densities  $\rho_{ac} = 0.419$  and  $0.324$ , respectively. For  $D \rightarrow 1$ , one recovers the limit of fully uncorrelated particles, so that  $P(\eta_0, \eta_1, \dots, \eta_{n-1}) = P(\eta_0, \eta_1)P(\eta_0, \eta_2)\dots P(\eta_0, \eta_{n-1})$ . In this limit, it follows that the transition takes place for  $\alpha_0 = 0.8154$  (black circle) with active phase density  $\rho_{ac} = 0.322$ . Despite displacing particles, mean-field results support that unlimited diffusion does not suppress the phase coexistence.

Fig. 1 (b) shows the phase diagram for the second approach for distinct weakening parameters  $p$ . As expected, by increasing  $p$  the phase coexistence becomes critical with a tricritical point  $T$  separating above regimes. However, MFT predicts a considerable fraction  $p_t = 0.80(1)$  to suppress the phase coexistence. Also, the phase diagram exhibits a reentrant shape for limited  $p$  and along the critical line  $p$  and  $\alpha$  presents a dependence about linear. Thus, unlike the diffusion, the competition between distinct creation mechanisms is able to suppress the phase coexistence.

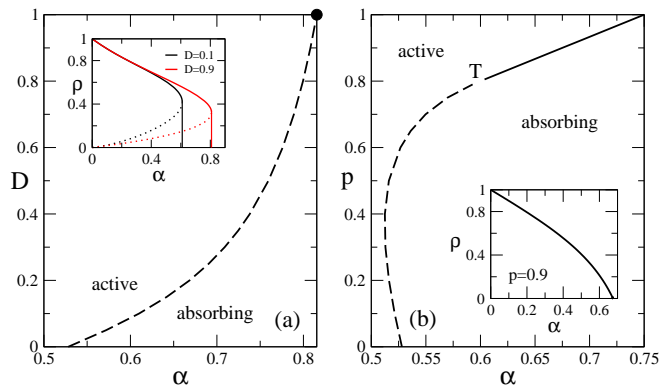


FIG. 1: Mean field phase diagrams for diffusive (a) and competitive models (b). Dashed and continuous lines denote discontinuous and continuous phase transitions, respectively. The black circle (a) indicates the transition point for  $D \rightarrow 1$  and  $T$  denotes the tricritical point (b). Left inset shows spinodal behaviors for  $D = 0.1$  and  $D = 0.9$ , whereas right inset shows the density  $\rho$  vs  $\alpha$  for  $p = 0.9$ .

## IV. NUMERICAL RESULTS

Numerical simulations have been performed for distinct system sizes and periodic boundary conditions. Due to the lack of a general theory for discontinuous absorbing transitions, distinct analysis will be presented.

In the first, we employ a similar finite size analysis than for equilibrium transitions. For instance, we apply the model dynamics together with the quasi-steady method [19]. Briefly, it consists of storing a list of  $M$  active configurations (here we store  $M = 2000$  configurations) and whenever the system falls into the absorbing state a configuration is randomly extracted from the list. The ensemble of stored configurations is continuously updated, where for each MC step a configuration belonging to the list is replaced with probability  $\tilde{p}$  (typically one takes  $\tilde{p} = 0.01$ ) by the actual system configuration, provided it is not absorbing. In particular, the ratio  $U_2 = \frac{\langle \rho^2 \rangle}{\langle \rho \rangle^2}$  is an useful quantity to characterize DP transitions, since its evaluation for distinct system sizes cross at the critical point  $\alpha_c$ , with the well defined value  $U_{2c} = 1.3257(5)$ . Conversely, discontinuous transitions are signed by bimodal probability distribution  $P_\rho$  (characterizing the absorbing and active phases) and also by a peak in the variance  $\chi = L^2[\langle \rho^2 \rangle - \langle \rho \rangle^2]$ . In equilibrium case,  $\chi$  scales with the system volume, whereas for nonequilibrium transitions, the scaling is still unknown. Here, we will also analyze the dependence of  $\chi$  on  $L$ , in order to compare it with the equilibrium case. Second, we study the time decay of the density  $\rho$  starting from a fully occupied lattice as initial configuration. As for critical and discontinuous phase transitions, for small  $\alpha$  the density  $\rho$  converges to a non null well defined value indicating endless activity, in which particles are continuously created and annihilated. On the contrary, for larger  $\alpha$ 's  $\rho$  vanishes exponentially toward a complete particle extinction. The coexistence point  $\alpha_0$  is the separatrix between above regimes, whereas at the critical point  $\alpha_c$   $\rho$  vanishes algebraically following a power-law behavior  $\rho \sim t^{-\theta}$ , with  $\theta$  its associated critical exponent. For the DP universality class it reads  $\theta = 0.4505(10)$ .

Figs. 2, 3 and 4 summarize results for the restrictive CP for three diffusion rates  $D = 0.1, 0.5$  and  $0.9$ . In all cases, the system density  $\rho$  vanishes in a short range of  $\alpha$  followed by a maximum of the variance  $\chi$  (panels (a) and their insets). For each diffusion value, the positions  $\alpha_L$ 's, (in which each  $\chi$  presents a maximum) scale with  $L^{-2}$  whereas the maximum of  $\chi$  increases with  $L^2$  (panels (b) and their insets). These results reveal that the scalings are similar to equilibrium discontinuous phase transitions [20, 21]. From this behavior, we obtain the estimates  $\alpha_0 = 0.2600(1)$  ( $D = 0.1$ ),  $0.3624(2)$  ( $D = 0.5$ ) and  $0.442(1)$  ( $D = 0.9$ ). These estimations agree with the values  $0.2590$ ,  $0.360$  and  $0.436$ , obtained from the time decay of  $\rho$  (panels (d)) for  $L = 150$ . Although the separatrix points exhibit finite size scaling corrections for smaller  $L$ 's, in all cases they seem to saturate for larger

system sizes (for  $L \geq 100$ , one already observes this).

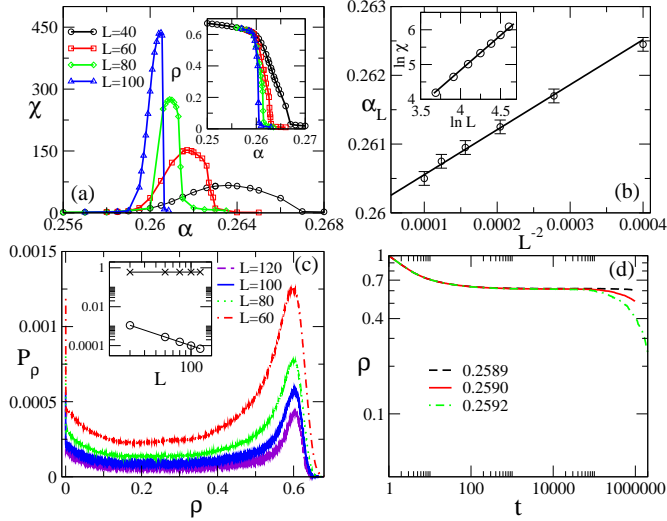


FIG. 2: For  $D = 0.1$ , panel (a) shows  $\chi$  and  $\rho$  (inset) vs  $\alpha$  for distinct system sizes  $L$ . In (b), the scaling plot of  $\alpha_L$ , in which  $\chi$  is maximum, vs  $L^{-2}$ . Inset shows the log-log plot of the maximum of  $\chi$  vs  $L$  and the straight line has slope 2. In (c) the quasi-stationary probability distribution  $P_\rho$  for  $L$ 's in which the peaks have the same height. In the inset, the log-log plot of the quasi-steady densities vs  $L$ . In (d) the time evolution of  $\rho$  for distinct  $\alpha$ 's.

Also, the order-parameter probability distributions  $P_\rho$  present bimodal shapes (panels (c)), with active phase densities  $\rho_{ac}$  converging to well defined values whereas  $\rho_{ab}$  vanishes algebraically as  $L$  increases (insets). For  $D = 0.1, 0.5$  and  $0.9$  the  $\rho_{ac}$ 's converge to  $0.603(1)$ ,  $0.501(2)$  and  $0.434(2)$ , respectively. For  $D = 0.99$  (not shown) a bimodal probability distribution with active phase centered at  $\rho_{ac} = 0.405(1)$  is observed. Thus, in similarity with MFT, numerical simulations show that clusters become less compact as  $D$  increases and the transition points move for larger annihilation values. Moreover, in contrast with results by Villa-Martin et al. [16], the phase coexistence is not suppressed for limited diffusion rates, although results agree qualitatively in the limit of intermediate and large diffusion regimes. Also, unlike the results by Guo et al. [10], all present analyses reveal that all discontinuous transitions take place in single and well defined points, in similarity with the equilibrium case and with previous results [11, 12].

Extending above analysis for distinct values of  $D$ , we obtain the phase diagram shown in Fig. 5.

To conclude, despite the qualitative agreement between MFT and numerical simulations, the shape of phase diagrams are different. Also, numerical results predict more compact clusters than MFT ones.

Next, we present results for the second approach, that are scrutinized in Figs. 6 and 7 for  $p = 0.1$  and  $p = 0.5$ , respectively. As for the diffusive case, panel (a) and its inset in Fig. 6 show that for  $p = 0.1$   $\rho$  vanishes in a tiny interval followed by peaks of  $\chi$ . Their po-

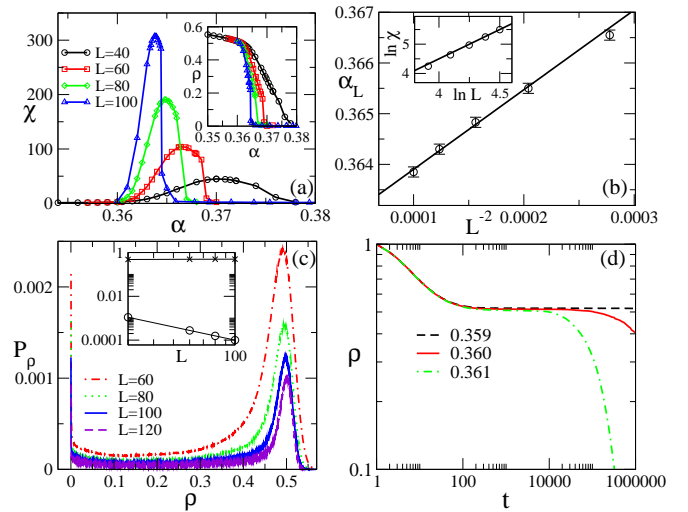


FIG. 3: For  $D = 0.5$  panel (a) shows  $\chi$  and  $\rho$  (inset) vs  $\alpha$  for distinct system sizes  $L$ . In (b), the scaling plot of  $\alpha_L$ , in which  $\chi$  is maximum, vs  $L^{-2}$ . Inset shows the log-log plot of the maximum of  $\chi$  vs  $L$  and the straight line has slope 2. In (c) the quasi-stationary probability distribution  $P_\rho$  for  $L$ 's in which the peaks have the same height. In the inset, the log-log plot of the quasi-steady densities vs  $L$ . In (d) the time evolution of  $\rho$  for distinct  $\alpha$ 's.

sitions exhibit similar dependence on the volume than previous diffusive results, from which we obtain the estimate  $\alpha_0 = 0.2377(2)$  (panel (b) and its inset). As previous cases, such value is close to  $0.2368$ , obtained from the separatrix point between the active and the exponential decay of  $\rho$  (panel (d)). Also, the existence of bimodal probability distributions, with active  $\rho_{ac}$  and absorbing  $\rho_{ab}$  densities behaving similarly than previous cases (panel (c) and its inset), reinforce a discontinuous transitions for  $p = 0.1$ . An entirely distinct behavior is verified for  $p = 0.5$  (Fig. 7). In particular,  $\rho$  vanishes in a broader interval of  $\alpha$  (panel (a)) and all curves for the ratio  $U_2$  (panel (b)) intersect at  $\alpha_c = 0.3848(3)$  with  $U_{2c} = 1.32(2)$ , in consistency with the DP value  $1.3257(5)$ . At  $\alpha_c$ , from the log-log plots of  $\rho$  vs  $L$  and  $\rho$  vs  $\Delta$  (where  $\Delta \equiv \alpha_c - \alpha$ ), we obtain the static critical exponents  $\beta/\nu_\perp = 0.79(1)$  and  $\beta = 0.58(1)$  (panel (c) and its inset), respectively. Such values agree very well with the DP values  $0.796(9)$  and  $0.5834(30)$ , respectively. Finally, in panel (d), we consider the time evolution of  $\rho$ . At  $\alpha_c$ ,  $\rho$  decays algebraically following an exponent consistent with the DP value  $0.4505(10)$ .

Extending above analysis for distinct values of  $p$  we obtain the phase diagram, shown in Fig. 8. The tricritical point separating discontinuous from continuous regime is located at  $(\alpha_t, p_t) = (0.277(8), 0.22(2))$ . Thus, in contrast with MFT, numerical results reveal that limited weakening parameter separates coexistence from the criticality. Also, the phase coexistence is not reentrant. Nevertheless, the threshold  $p_t$  is quite larger than the value  $p_t \sim 0.032$  obtained by Guo et al. [17], suggesting

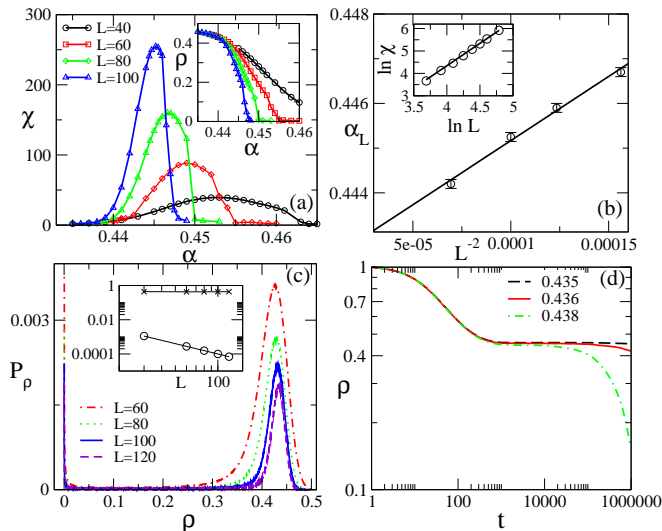


FIG. 4: For  $D = 0.9$ , panel (a) shows  $\chi$  and  $\rho$  (inset) vs  $\alpha$  for distinct system sizes  $L$ . In (b), the scaling plot of  $\alpha_L$ , in which  $\chi$  is maximum, vs  $L^{-2}$ . Inset shows the log-log plot of the maximum of  $\chi$  vs  $L$  and the straight line has slope 2. In (c) the quasi-stationary probability distribution  $P_\rho$  for  $L$ 's in which the peaks have the same height. In the inset, the log-log plot of the quasi-steady densities vs  $L$ . In (d) the time evolution of  $\rho$  for distinct  $\alpha$ 's.

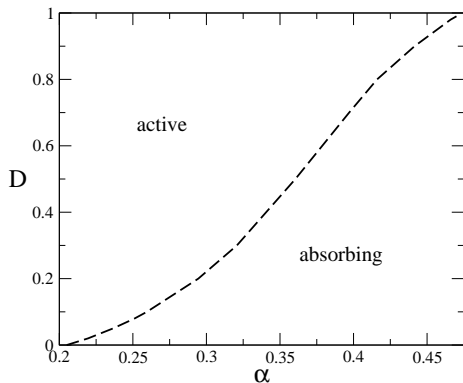


FIG. 5: The phase diagram in the plane  $D - \alpha$  obtained from MC simulations. Dashed line denotes discontinuous phase transitions.

that the simplest studied restrictive model prolongs the phase coexistence [22].

## V. CONCLUSIONS

To sum up, we studied the influence of two distinct dynamics in the simplest model exhibiting a discontinuous absorbing phase transition. They have been studied via mean-field analysis and distinct numerical simulations. Results show that although the inclusion of a

weakening restrictive dynamics suppresses the phase coexistence (for intermediate and large rates), this is not

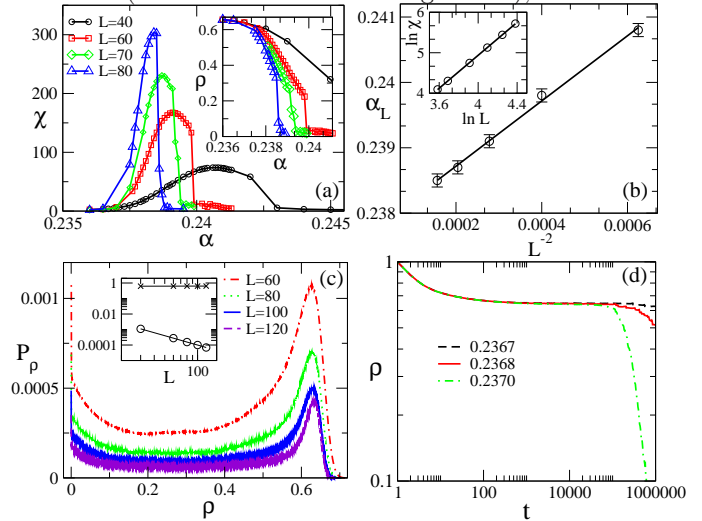


FIG. 6: For  $p = 0.1$ , panel (a) shows  $\chi$  and  $\rho$  (inset) vs  $\alpha$  for distinct system sizes  $L$ , respectively. In (b), the scaling plot of  $\alpha_L$ , in which  $\chi$  is maximum, vs  $L^{-2}$ . Inset shows the log-log plot of the maximum of  $\chi$  vs  $L$  and the straight line has slope 2. In (c) the quasi-stationary probability distribution  $P_\rho$  for  $L$ 's in which the peaks have the same height. In the inset, the log-log plot of the quasi-steady densities vs  $L$ . In (d) the time evolution of  $\rho$  for distinct  $\alpha$ 's.

the case of the diffusion, in which the phase coexistence is maintained for all values. These results are distinct from those obtained in Refs. [10, 16], in which limited diffusion induces a critical transition and the generic two-phase coexistence disappears by increasing  $D$ , respectively. Thus our results reveal not only an additional feature of diffusion, but also the differences between lattice model and Langevin approaches. Other remarkable result concerns that all studied discontinuous transitions present a finite size scaling behavior similar to the equilibrium phase transitions, in which relevant quantities scale with the system volume. Although further studies are still required, these results rise the possibility of a general scaling for nonequilibrium phase transitions.

## ACKNOWLEDGMENT

The authors wish to thank Brazilian scientific agencies CNPq, INCT-FCx for the financial support. Salette Pianegonda also wishes to thank the Physics Department of the Federal Technological University, Paraná (DAFIS-CT-UTFPR) for providing the access to its high-performance computer facility. We also acknowledge M. A. Muñoz for providing us the preprint [16] before the publication.

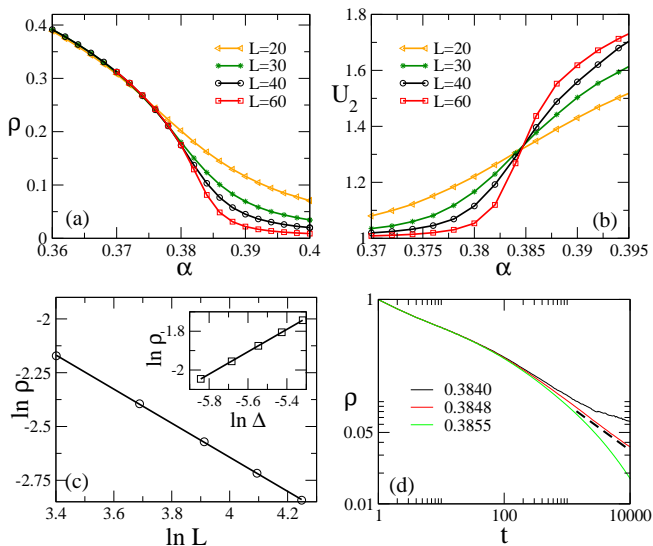


FIG. 7: For  $p = 0.5$ , panels (a) and (b) show  $\rho$  and  $U_2$  vs  $\alpha$  for distinct system sizes  $L$ , respectively. In (c) we show the log-log plot of  $\rho$  vs  $L$  and  $\Delta = \alpha_c - \alpha$  (inset). The slopes read  $\beta/\nu_{\perp} = 0.79(1)$  and  $\beta = 0.58(1)$  (inset) and  $\alpha_c = 0.3848(3)$ . Part (d) shows the time evolution of  $\rho$  for distinct  $\alpha$ 's. The straight line as slope  $0.4505(10)$ .

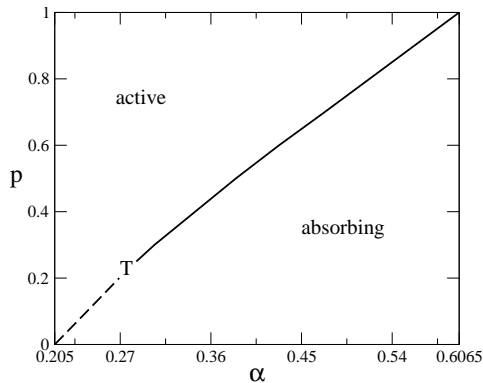


FIG. 8: The phase diagram in the plane  $p - \alpha$  obtained from MC simulations. Dashed and continuous lines denote discontinuous and continuous phase transitions, respectively, and  $T$  is the tricritical point.

- 
- [1] J. Marro and R. Dickman, Nonequilibrium Phase Transitions in Lattice Models (Cambridge University Press, Cambridge, England, 1999).
- [2] G. Odor, Rev. Mod. Phys. **76**, 663 (2004).
- [3] K. A. Takeuchi, M. Kuroda, H. Chaté and M. Sano, Phys. Rev. Lett. **99**, 234503 (2007).
- [4] L. Corté, P. M. Chaikin, J. P. Gollub and D. J. Pine, Nat. Phys. **4**, 420 (2008).
- [5] S. Okuma, Y. Tsugawa and A. Motohashi, Phys. Rev. B **83**, 012503 (2011).
- [6] T. E. Harris, Ann. Probab. **2**, 969 (1974).
- [7] F. Schlögl, Z. Phys. **253**, 147 (1972).
- [8] R. M. Ziff, E. Gulari and Y. Barshad, Phys. Rev. Lett. **56**, 2553 (1986).
- [9] Da-Jiang Liu, Xiaofang Guo and J. W. Evans, Phys. Rev. Lett. **98**, 050601 (2007).
- [10] Xiaofang Guo, Da-Jiang Liu and J. W. Evans, J. Chem. Phys. **130**, 074106 (2009).
- [11] E. F. da Silva and M. J. de Oliveira, J. Phys. A **44**, 135002 (2011).
- [12] C. E. Fiore, Phys. Rev. E **89**, 022104 (2014).
- [13] C. Varghese and R. Durrett, Phys. Rev. E **87**, 062819 (2013).
- [14] V. Elgart and A. Kamenev, Phys. Rev. E **74**, 041101

- (2006).
- [15] P. Villa Martín, J. A. Bonachela and M. A. Muñoz, Phys. Rev. E **89**, 012145 (2014).
- [16] P. Villa Martín, J. A. Bonachela and M. A. Muñoz, in press.
- [17] Xiaofang Guo, D. K Unruh, Da-Jiang Liu and J. W. Evans, Physica A **391**, 633 (2012).
- [18] M. M. Sabag and M. J. de Oliveira, Phys. Rev. E **66**, 036115 (2002).
- [19] M. M. de Oliveira and R. Dickman, Phys. Rev. E **357**, 016129 (2005).
- [20] C. Borgs and R. Kotecký, J. Stat. Phys. **61**, 79 (1990); *ibid*, Phys. Rev. Lett. **68**, 1734 (1992).
- [21] C. E. Fiore and M. G. E. da Luz, Phys. Rev. Lett. **107**, 230601 (2011).
- [22] The parameter  $\delta$  considered in [17] are related to  $p$  through relation  $p = \frac{\delta}{1+\delta}$ .